*J. Astrophys. Astr.* (2018) 39:6
https://doi.org/10.1007/s12036-018-9511-z



*Review*

# A comparative study of single-temperature and two-temperature accretion flows around black holes

INDU KALPA DIHINGIA[1,*], SANTABRATA DAS[1] and SAMIR MANDAL[2]

[1]Indian Institute of Technology Guwahati, Guwahati 781 039, India.
[2]Indian Institute of Space Science and Technology, Thiruvananthapuram 695 547, India.
*Corresponding author. E-mail: i.dihingia@iitg.ernet.in

MS received 11 September 2017; accepted 4 January 2018; published online 9 February 2018

**Abstract.** We study the properties of sub-Keplerian accretion disk around a stationary black hole, considering bremsstrahlung, synchrotron and Comptonization of synchrotron photons as radiative cooling mechanisms active in the disk. We obtain the solutions of two-temperature global accretion flow (TTAF) and compare it with the results obtained from single-temperature (STAF) model. We observe that flow properties, in particular, the radial profile of electron and ion temperatures differ noticeably in the adopted models for flows with identical boundary conditions fixed at the outer edge of the disk. Since the electron temperature is one of the key factors to regulate the radiative processes, we argue that physically motivated description of electron temperature needs to be considered in studying the astrophysical phenomena around black holes.

**Keywords.** Black holes—hydrodynamics—shock waves.

## 1. Introduction

The time scales of physical phenomena inside a system play a crucial rule on the observed properties of that system. In an accretion disk, the constituent electrons and ions collide due to the random thermal motion. During collision, energy is being exchanged between the electrons and ions following the physical mechanism of Coulomb collision and eventually thermal equilibrium is achieved in an accreting plasma. However, when the bulk motion of the inflowing matter is significantly large, the in-fall time scale becomes much shorter than that of the ion–electron collision timescale. Therefore, it becomes difficult to maintain perfect thermal equilibrium between ions and electrons. Hence, the existence of a single-temperature flow seems to be unlikely, instead accretion flow prefers the two-temperature attire, especially at the inner part of the disk.

In order to understand the hard X-ray spectra of black hole (BH) candidate Cyg-X1, Shapiro *et al.* (1976) suggested the two-temperature accretion flow model. This model has been widely studied and applied to X-ray binaries (XRBs) and active galactic nuclei (AGNs) (Kusunose & Takahara 1988, 1989; White & Lightman 1989; Wandel & Liang 1991; Luo & Liang 1994) although Pringle (1976) and Piran (1978) reported that SLE model is thermally unstable. Later it is shown that the thermal instability disappears when the advection is present in the flow. In the presence of advection, Chakrabarti & Titarchuk (1995b) and Mandal & Chakrabarti (2005) modeled two-temperature accretion flow and emphasized the possibility of shock in it. But, their model was not in accordance with self-consistent hydrodynamics. Based on the above scenario, in this work, we investigate the properties of the two-temperature accretion flow (TTAF) around black holes considering the relevant radiative processes, namely, bremsstrahlung, synchrotron, and Compton cooling. Interestingly, when rotating flow accretes towards the black hole, it experiences centrifugal repulsion against gravity that causes the slowing down of inflowing matter. With this, matter accumulates in the vicinity of the black hole and forms a virtual barrier around the black holes. Eventually, depending on the flow parameters, such a barrier triggers the discontinuous transition of flow variables in the form of shock waves. Since the post-shock flow is hot and dense, it generates hard radiations that are commonly observed from black hole sources. Hence, the hydrodynamic characteristics of the post-shock region will

possibly be responsible to explain the spectral properties of the black hole candidates. Thus, in this work, we also study the properties of shock waves in terms of flow parameters. Further, we continue our study considering the single temperature accretion flow model (STAF) and compare the results with the shock-induced global accretion solution of TTAF. It is to be mentioned that in STAF, ion temperature is calculated self-consistently, but electron temperature is estimated from the ion temperature using the scaling relation as $T_e = \sqrt{m_e/m_p}T_p$ (Chattopadhyay & Chakrabarti 2002).

The rest of the paper is organized as follows: In section 2, we present model equations and solution methodology. In section 3, we discuss the obtained results. Finally, in section 4, we present a discussion and summary of our work.

## 2. Model equations

### 2.1 *Basic hydrodynamics*

We study TTAF by considering a steady, thin, axisymmetric and viscous accreting matter around a Schwarzschild black hole. The space time geometry around the central black hole is approximated by adopting a pseudo Newtonian potential. The form of the potential in cylindrical coordinate is given by $\Phi = -GM_{\rm BH}/(r - 2GM_{\rm BH}/c^2)$ (Paczynsky & Wiita 1980), where $G$ is the gravitational constant, $M_{\rm BH}$ is the mass of the black hole, $c$ is the speed of light and $r$ is the radial coordinate. We use natural unit system where $2G = M_{\rm BH} = c = 1$. In this unit system, radial coordinate, angular momentum and radial velocity is expressed in units of $2GM_{\rm BH}/c^2$, $2GM_{\rm BH}/c$ and $c$, respectively. Throughout the study, we consider the mass of the black hole as $10M_\odot$ unless otherwise stated, where $M_\odot$ represents solar mass.

In the steady state, the governing equations for accreting matters are given by

(a) Mass conservation equation

$$\dot{M} = 2\pi\Sigma x u, \tag{1}$$

(b) Radial momentum equation

$$u\frac{{\rm d}u}{{\rm d}x} + \frac{1}{\rho}\frac{{\rm d}P}{{\rm d}x} - \frac{\lambda^2}{x^3} + \frac{{\rm d}\Phi}{{\rm d}x} = 0, \tag{2}$$

(c) Azimuthal momentum equation

$$u\frac{{\rm d}\lambda}{{\rm d}x} + \frac{1}{\Sigma x}\frac{\rm d}{{\rm d}x}\left(x^2 W_{x\phi}\right) = 0, \tag{3}$$

where $x$, $u$, $P$, $\lambda$, $\dot{M}$, $\rho$ and $\Sigma$ represent the radial distance, radial velocity, isotropic pressure, specific angular momentum, accretion rate, volume mass density and surface mass density, respectively. Here, $W_{x\phi}$ $(= -\alpha\Pi)$ is the viscous stress, where $\alpha$ is the viscosity parameter and $\Pi$ $(= W + \Sigma u^2)$ is the vertically integrated total pressure (Chakrabarti and Molteni 1995a) and $W$ is the vertically integrated gas pressure (Matsumoto *et al.* 1984). Moreover, in this work, we express the accretion rate ($\dot{m}$) in units of Eddington rate ($\dot{M}_{\rm Edd}$) throughout the paper.

(d) Finally, the entropy generation equations for ions and electrons are

$$\frac{u}{\gamma_i - 1}\left(\frac{1}{\rho_i}\frac{{\rm d}P_i}{{\rm d}x} - \frac{\gamma_i P_i}{\rho_i^2}\frac{{\rm d}\rho_i}{{\rm d}x}\right) = \frac{Q_i^- - Q_i^+}{\rho_i} \tag{4a}$$

and

$$\frac{u}{\gamma_e - 1}\left(\frac{1}{\rho_e}\frac{{\rm d}P_e}{{\rm d}x} - \frac{\gamma_e P_e}{\rho_e^2}\frac{{\rm d}\rho_e}{{\rm d}x}\right) = \frac{Q_e^- - Q_e^+}{\rho_e}, \tag{4b}$$

where the quantities for ions and electrons are represented by the subscripts $i$ and $e$. And, $\gamma_{i,e}$ is the ratio of specific heats, $Q_{i,e}^+$ is the dimensionless total heating terms and $Q_{i,e}^-$ is the dimensionless total cooling terms of the ions and electrons, respectively. The ratio of specific heats for thermally non-relativistic ions is taken to be $\gamma_i = 3/2$ and the same for thermally relativistic electrons is taken to be $\gamma_e = 4/3$. For single temperature flow, ions and electrons remain coupled and therefore, we have single entropy generation equation which is given by

$$\frac{u}{\gamma - 1}\left(\frac{1}{\rho}\frac{{\rm d}P}{{\rm d}x} - \frac{\gamma P}{\rho^2}\frac{{\rm d}\rho}{{\rm d}x}\right) = \frac{Q^- - Q^+}{\rho}, \tag{4c}$$

where all the quantities have their usual meaning. Here, we use $\gamma = 3/2$. Further, we define the sound speed as $a = \sqrt{P/\rho}$, where $P$ denotes the total pressure. For two-temperature flow, total pressure is obtained as $P = P_i + P_e$.

According to Chakrabarti and Molteni (1995a), the heating of ions due to viscosity is given by

$$\frac{Q_i^+}{\rho_i} = \Gamma_i = -2\alpha I_n x\left(g a^2 + u^2\right)\frac{{\rm d}\Omega}{{\rm d}x}. \tag{5}$$

where $g = I_{n+1}/I_n$, $I_n = (2^n n!)^2/(2n+1)!$ (Matsumoto *et al.* 1984), $n = 1/(\gamma_i - 1)$ and $\Omega$ is the angular velocity of the flow. The ions cool due to the transfer of energy from the ions to electrons via Coulomb collision ($Q_{ei}$) and through the inverse bremsstrahlung of

the ions ($Q_{ib}$). Therefore, the total cooling rate of ions is given by (Colpi *et al.* 1984; Mandal & Chakrabarti 2005; Spitzer 2013)

$$Q_i^- = Q_{ei} + Q_{ib}. \tag{6}$$

Through the Coulomb collision, electrons get energy from ions and heats up. Therefore, we have

$$Q_e^+ = Q_{ei}. \tag{7}$$

The thermally relativistic electrons respond efficiently to bremsstrahlung ($Q_b$), cyclo-synchrotron ($Q_{cs}$), and Comptonization ($Q_{mc}$) cooling processes. Thus, the total electron cooling is given by (Rybicki & Lightman 1979; Mandal & Chakrabarti 2005)

$$Q_e^- = Q_b + Q_{cs} + Q_{mc}. \tag{8}$$

In the present work, due to simplicity, we consider stochastic magnetic fields and approximate that the ratio of the magnetic pressure to the gas pressure remains constant throughout the accretion disk. With this, we define ($\beta$) as

$$\beta = \frac{B^2/8\pi}{P}. \tag{9}$$

In general, $\beta \lesssim 1$, this approximation ensures the confinement of the magnetic fields within the accretion disk. Throughout the study, we consider $\beta = 0.1$.

### 2.2 *Solution methodology*

The accretion solution around the black hole must be transonic in nature as flow velocity at the outer edge is negligibly small whereas flow must cross the black hole horizon with velocity comparable to the speed of light. Thus, any acceptable solution must contain sonic point (where flow changes its sonic state from subsonic to supersonic). Depending on the flow parameters, flow can have multiple sonic points. When sonic point forms close to the horizon, it is known as inner sonic point ($x_{\rm in}$) and when it forms far away from the black hole, it is called as outer sonic point ($x_{\rm out}$). Accretion flow must pass either one of these two sonic points or through both the sonic points, with a shock transition in between (Fukue 1987; Chakrabarti 1989). In general, inflowing matter starts accreting with negligible radial velocity from the outer edge of the disk. During the accretion process, flow crosses the outer sonic point to become supersonic and continue to move towards the black hole. Eventually, centrifugal repulsion becomes significant and flow encounters shock transition in the subsonic branch. Here, flow momentarily slows down and again gains its radial velocity due to strong gravitational attraction as it moves towards the black hole. Finally, flow enters into the black hole supersonically after crossing the inner sonic point.

At the shock, flow variables experience a discontinuous transition. These transitions are characterized by the Rankine–Hugoniot conditions which are given by (a) conservation of mass flux: $\dot{m}_+ = \dot{m}_-$, (b) energy flux: $\mathcal{E}_+ = \mathcal{E}_-$, and (c) momentum: $W_+ + \Sigma_+ u_+^2 = W_- + \Sigma_- u_-^2$, respectively. Here, '$-$' and '$+$' denote the quantities immediately before and after the shock transition.

For two-temperature flow, the relaxation time for electron–electron collision is usually much shorter than that of either electron–ion or ion–ion relaxation time. Hence, we assume that the temperature of the electrons remain unaffected across the shock front and we have $T_{e+} = T_{e-}$.

## 3. Results

### 3.1 *Global solutions for TTAF*

In order to get the global accretion solutions of TTAF, we simultaneously solve equations (1), (2), (3), (4a), (4b) by suppling viscosity ($\alpha$) and accretion rate ($\dot{m}$), along with the inner sonic point location $x_{\rm in}$, the angular momentum at the inner sonic point $\lambda_{\rm in}$ and electron temperature $T_{e,\rm in}$. In Fig. 1, we present the obtained result where Mach number is plotted against logarithmic radial distance. The solid curve represents accretion branch and the dashed curve denotes the wind branch. The variation of solution topologies under variation of $x_{\rm in}$ and $\lambda_{\rm in}$ is well-known for viscous transonic flow (e.g. Chakrabarti 1996), but not tested in TTAF. In the upper panel, we fix $T_{e,\rm in} = 1\times10^{10}$ K, $\lambda_{\rm in} = 1.545, \alpha = 0.01$, $\dot{m} = 0.001$ and vary inner sonic point location ($x_{\rm in}$). As the sonic point location moves away from the BH (as (a) $x_{\rm in} = 2.70$, (b) $x_{\rm in} = 2.765$ and (c) $x_{\rm in} = 2.80$), an open topology connecting the outer edge of the disk and the black hole horizon gradually becomes a closed one which apparently fails to represent a complete global accretion solution. As these solutions can not connect to the outer edge of the disk with the event horizon, they are not physically acceptable solutions. Earlier, open solutions of type (a) were studied by Narayan & Yi (1995), Manmoto *et al.* (1997) and Rajesh & Mukhopadhyay (2010). The close solution of types (b) and (c) can be part of the accretion solution provided it is connected to another solution passing through the outer sonic point via shock transition. In case of (b), shock conditions are favorable and therefore we obtain a global solution

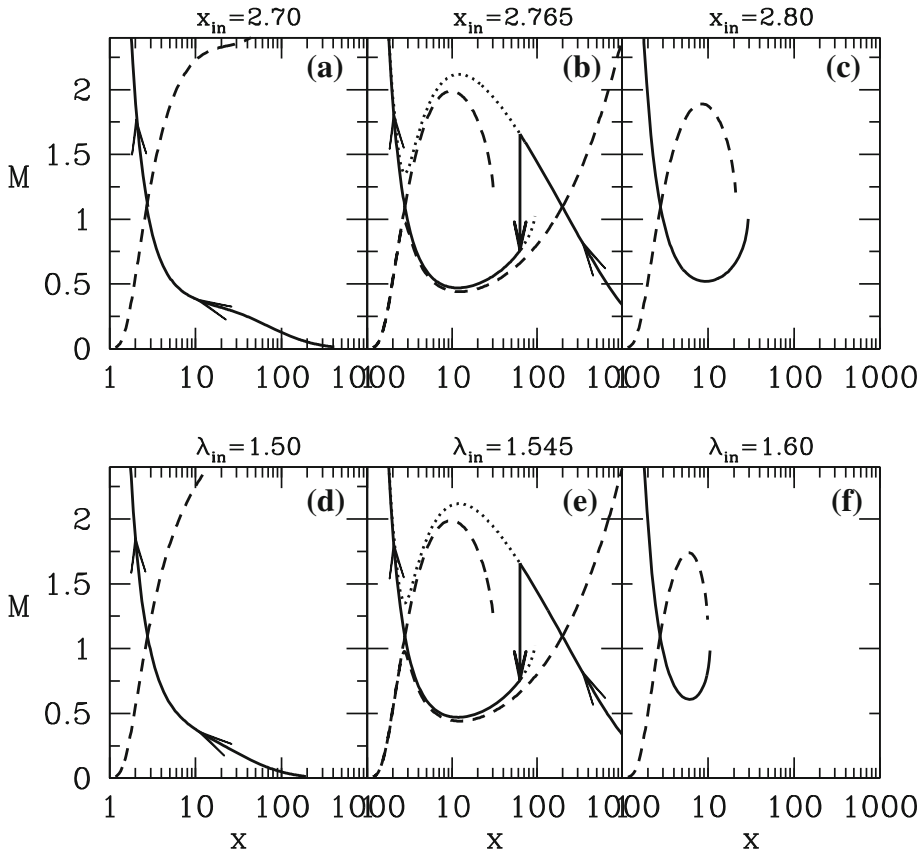


**Figure 1.** Variation solution topology for accretion and wind with change in inner sonic point location ($x_{\rm in}$) **(a)–(c)** and angular momentum at the inner sonic point ($\lambda_{\rm in}$) **(d)–(f)**. The solid line represents the solutions for accretion and dashed line represents wind solutions. See text for details.

containing the shock for TTAF. Here, flow encounters shock transition at $x_s = 62.810$ which is indicated by the vertical downward arrow and overall, the arrows indicate the direction of flow motion towards the black hole. The solutions of these kind are recently studied by Dihingia *et al.* (2015, 2017). Incidentally, in the case of solution of type (c), shock conditions are not satisfied and therefore, it can not be considered as a physically acceptable solution.

Similarly, in the lower panel of Fig. 1, we choose $T_{e,\rm in} = 1 \times 10^{10}$ K, $\alpha = 0.01$, $\dot{m} = 0.001$ and $x_{\rm in} = 2.765$ and vary $\lambda_{\rm in}$. For panel (d), (e) and (f), we fix $\lambda_{\rm in}$ as 1.50, 1.545 and 1.60 respectively. As before, we obtain a global accretion solution that is shown in panel (d). The result plotted in panel (e) is identical to panel (b) which we obtain when angular momentum is increased from 1.50 to 1.545 while keeping all the remaining flow parameters unaltered. When $\lambda_{\rm in}$ is increased further, shock disappears. This indicates that there exist ranges of $x_{\rm in}$ and $\lambda_{\rm in}$ that allow global shock solutions. Accordingly, we separate the region of parameter space spanned by the energy at the inner sonic point ($\mathcal{E}_{\rm in}$) and $\lambda_{\rm in}$ that allows shock-induced global TTAF solutions. Here, we have $\mathcal{E}(x) = 0.5u^2 + \gamma_i a^2/(\gamma_i - 1) + 0.5\lambda^2/x^2 - 0.5/(x-1)$.

### 3.2 *Parameter space for shock in TTAF*

In order to examine the influence of flow parameters on the TTAF solutions, we calculate the parameter space in the $\lambda_{\rm in} - \mathcal{E}_{\rm in}$ plane that allows standing shock solutions. In Fig. 2, we show the modification of parameter space ($\lambda_{\rm in} - \mathcal{E}_{\rm in}$) for flows with different $\alpha$. Here, solid and dotted curves are obtained for $\alpha = 0$ and 0.01, respectively. The other flow parameters are chosen as $\dot{m} = 0.01$ and $T_{e,\rm in} = 6.75 \times 10^9$ K. On the one hand, viscosity transports angular momentum outward enabling the advective flow to accrete, and on the other hand, it helps to increase the flow energy due to viscus dissipation. As a result, shock parameter space for a viscous flow is shifted towards the higher energy and lower angular momentum domain compared to the inviscid case. In

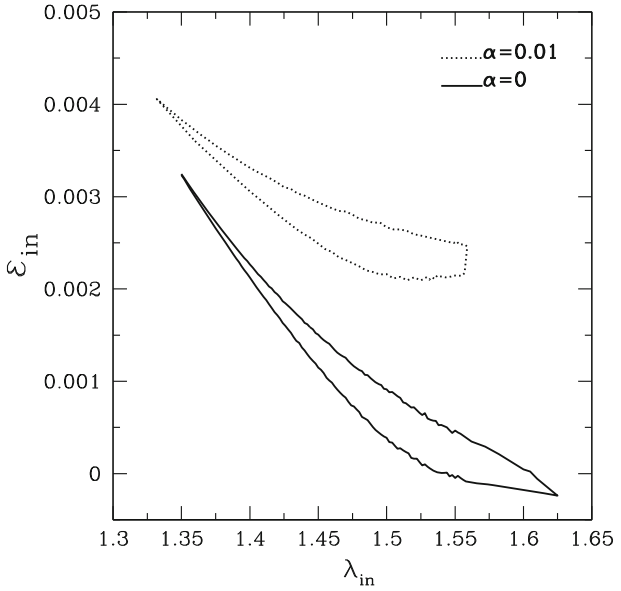


**Figure 2.** $\mathcal{E}_{in} - \lambda_{in}$ parameter space for shock in TTAF model. The region bounded by the solid and dotted curves are for $\alpha = 0$ and 0.01, respectively. See text for details.

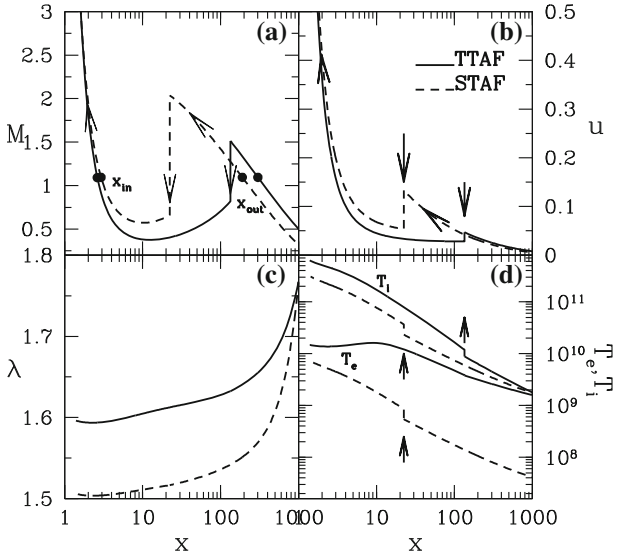


**Figure 3.** Comparison of **(a)** Mach number, **(b)** radial velocity, **(c)** angular momentum, and **(d)** temperature profiles for TTAF and STAF models. Here, we choose same sets of input parameters fixed at the outer edge of the disc. See text for details.

Fig. 2, similar features are depicted which are in agreement with the results of STAF (Das & Chakrabarti 2004; Das 2007).

### 3.3 *Comparison of STAF and TTAF including shock*

In the context of disc dynamics, since the TTAF model is developed with more physical reasoning than the STAF model, it is worth comparing the shocked accretion solutions obtained from both the models. Thus, in Fig. 3, we present the global accretion solutions including shock waves where results depicted using solid and dashed curves are for TTAF and STAF, respectively. Here, we inject matter from the outer edge of the disc as $x_{\rm edge} = 1000$ with $\lambda_{\rm edge} = 1.768$, $T_{i,\rm edge} = 1.588 \times 10^9$ K, $\dot{m} = 0.01$ and $\alpha = 0.005$, respectively. In Fig. 3a, we display the variation of Mach number ($M$) with the radial co-ordinate. The filled circles indicate the inner and outer sonic point locations which are marked in the figure. Subsonic matter from the outer edge of the disc starts accreting due to gravitational attraction. Inflowing matter crosses the outer sonic point ($x_{\rm out}$) to become supersonic and continue its journey towards black hole. Eventually, centrifugal repulsion becomes significant and that triggers the flow to jump in the subsonic branch while passing through the shock wave. Subsequently, flow continues to accrete as it gains its radial velocity again and enters into the black hole supersonically after passing through the inner sonic point ($x_{\rm in}$). In the figure, vertical arrows denote the location of shock transitions and overall, arrows indicate the direction of the flow motion towards the black hole. Note that results obtained from TTAF and STAF are very much different as the location of the shock transitions in these two cases are far apart. This happens due to the fact that in order to obtain the shocked accretion solution, we need to choose different local energy of the flow for TTAF and STAF model which are given by $\mathcal{E}^{\rm TTAF}_{\rm edge} = 3.160 \times 10^{-4}$ and $\mathcal{E}^{\rm STAF}_{\rm edge} = 4.896 \times 10^{-4}$. This essentially indicates that it is not possible to obtain the same shocked accretion solutions in STAF model using the TTAF model parameters. In other wards, no correspondence exists between the flow parameters of TTAF and STAF models. In Fig. 3b, we show the velocity profile of global accretion solutions corresponding to the results presented Fig. 3a. Significant difference is observed in the radial velocity profile. However, in all cases, radial velocity jumps from supersonic to subsonic value which is indicated by vertical arrows directed downward. In Fig. 3c, we depict how the angular momentum is varied with radial coordinate inside the disc in both the models. These results correspond to the accretion solutions presented in Fig. 3a. We find that although flow starts with same $\lambda_{\rm edge}$ and $\alpha$ in both the models, angular momentum deviates from each other. This happens due to the fact that total pressure (thermal and ram) of the flow in these two models are different because of their dissimilar local

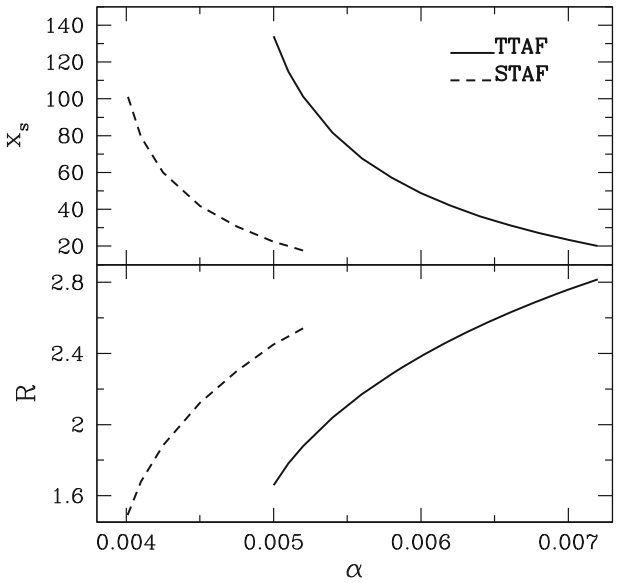


**Figure 4.** The variation of shock location ($x_s$) and compression ratio ($R$) with viscosity parameter for TTAF and STAF model. See text for details.

flow energy and therefore, the flow experiences different viscous stress resulting in a distinguishable angular momentum profile. In Fig. 3d, we show the variation of electron and ion temperatures with radial coordinate for flows with identical parameters as in Fig. 3a. It is clear that electron and ion temperatures in STAF models maintain the scaling relation between them throughout which is absent in the results of the TTAF model. Based on the above observations, it is quite evident that TTAF model is superior over STAF model as the former provides self-consistent two-temperature shocked accretion solutions. Therefore, solutions obtained from TTAF model would be more reliable in order to explain the observed spectral and timing properties of the black hole candidates.

In Fig. 4, we examine the effect of viscosity on the shock dynamics and shock properties. While doing this, we inject flow from $x_{\rm edge} = 1000$ with $\lambda_{\rm edge} = 1.768$, $T_{i,\rm edge} = 1.588 \times 10^9$ K and $\dot{m} = 0.01$, respectively. Here, results plotted with solid and dashed curves are for TTAF and STAF models. As viscosity is increased, in all models, the transport of angular momentum is enhanced and that weakens the centrifugal support of the flow against gravity. Hence, the shock front moves towards the BH in order to maintain pressure balance across the shock front (Fig. 4a). From the figure, it is clear that the range of viscosity for two different models are very much distinguishable although the rest of the flow parameters remain the same. Further, we calculate the compression ratio ($R$) that eventually measures the density compression across the shock front. In Fig. 4b, we show the variation of $R$ with $\alpha$. As shock front moves towards the BH, flow experiences a higher gravitational compression at the shock. So, higher viscosity parameter demands a highly compressed and smaller post-shock region, and we observed that $R$ increases with the increase of $\alpha$.

## 4. Discussion and summary

In this work, we describe the methodology to study TTAF around a Schwarzschild BH in the presence of relevant radiative processes, namely, bremsstrahlung, synchrotron and Comptonization of synchrotron photons. We obtain the shock-induced global two-temperature accretion solutions for a wide range of flow parameters. To establish our claim, we study the parameter space spanned by $\lambda_{\rm in}$ and $\mathcal{E}_{\rm in}$ that allows shock waves and find that effective region of the shock parameter space is quite large. When viscosity is increased, effect of dissipation is also increased in the flow which is evidently reflected in the shock parameter space as it is shifted to the high energy and low angular momentum domain (Fig. 2).

Next, we compare global accretion solutions including shock waves for TTAF and STAF models for the same set of flow parameters fixed at the outer edge of the disc. In order to obtain shock in both the models, we chose different local energies of the flow and different shock locations. Since the post-shock flow (i.e., PSC) is hot and dense, soft photons from the disc are intercepted at PSC that reprocessed the soft-photon via inverse Comptonization process to generate hard radiations. Therefore, the size of PSC has a key role in the process of hard photon emission from the disk.

We show the variation of shock location and compression ratio with viscosity parameters. Since the spectral properties depend on these quantities, any change in these quantities would lead to change in spectral state of the BH (Mandal & Chakrabarti 2005). The spectral state transition of BH is a quite commonly observed phenomenon (e.g. Belloni *et al.* 2006; Gierliński & Newton 2006; Miyakawa *et al.* 2008). While modeling such transitions, the temperature of ions and electrons should be calculated self-consistently. Otherwise, a simple-minded approximation may take one to a completely different domain of parameter space (Fig. 3). In this respect, we give emphasis to the TTAF model over the STAF model as it provides physically motivated realistic accretion solutions including shock waves.

## References


Belloni T. *et al.* 2006, MNRAS, 367, 1113
Chakrabarti S. K. 1989, ApJ, 347, 365
Chakrabarti S. K., Molteni D. 1995, MNRAS, 272, 80
Chakrabarti S., Titarchuk L. G. 1995, ApJ, 455, 623
Chakrabarti S. K. 1996, ApJ, 464, 664
Chattopadhyay I., Chakrabarti S. K. 2002, MNRAS, 333, 454
Colpi M., Maraschi L., Treves A. 1984, ApJ, 280, 319
Das S. 2007, MNRAS, 376, 1659
Das S., Chakrabarti S. K. 2004, Int. J. Mod. Phys. D, 13, 1955
Dihingia I., Das S., Mandal S. 2015, in Astronomical Society of India Conference Series, Volume 12
Dihingia I., Das S., Mandal S. 2017, MNRAS, in press
Fukue J. 1987, Publ. Astron. Soc. Japan, 39, 309
Gierliński M., Newton J. 2006, MNRAS, 370, 837
Kusunose M., Takahara F. 1988, Publ. Astron. Soc. Japan, 40, 435
Kusunose M., Takahara F. 1989, Publ. Astron. Soc. Japan, 41, 263
Luo C., Liang E. P. 1994, MNRAS, 266, 386
Mandal S., Chakrabarti S. K. 2005, A&A, 434, 839
Manmoto T., Mineshige S., Kusunose M. 1997, ApJ, 489, 791
Matsumoto R., Kato S., Fukue J., Okazaki A. T. 1984, Publ. Astron. Soc. Japan, 36, 71
Miyakawa T., Yamaoka K., Homan J., Saito K., Dotani T., Yoshida A., Inoue H. 2008, Publ. Astron. Soc. Japan, 60, 637
Narayan R., Yi I. 1995, ApJ, 452, 710
Paczynsky B., Wiita P. J. 1980, A&A, 88, 23
Piran T. 1978, ApJ, 221, 652
Pringle J. 1976, MNRAS, 177, 65
Rajesh S., Mukhopadhyay B. 2010, MNRAS, 402, 961
Rybicki G. B., Lightman A. P. 1979, Radiative Processes in Astrophysics, Wiley-Interscience
Shapiro S. L., Lightman A. P., Eardley D. M. 1976, ApJ, 204, 187
Spitzer L. 2013, Physics of fully ionized gases, Courier Corporation
Wandel A., Liang E. P. 1991, ApJ, 380, 84
White T. R., Lightman A. P. 1989, ApJ, 340, 1024